PLEASE CITE THIS ARTICLE AS DOI: 10.1116/6.0002580

7.5 kV, 6.2 GW.cm⁻² NiO/β-Ga₂O₃ Vertical Rectifiers with On-Off ratio greater than 10¹³

Running title: 7.5 kV NiO/β-Ga₂O₃ Vertical Rectifiers

Running Authors: Li et al.

Jian-Sian Li¹, Chao-Ching Chiang¹, Xinyi Xia¹, Hsiao-Hsuan Wan¹, Fan Ren¹ and S.J. Pearton^{2,a)}

Department of Chemical Engineering, University of Florida, Gainesville, FL 32606 USA
 Department of Materials Science and Engineering, University of Florida, Gainesville, FL 32606 USA

a) Electronic mail: spear@mse.ufl.edu

Vertical geometry NiO/ β n-Ga₂O/n⁺ Ga₂O₃ heterojunction rectifiers with contact sizes from 50-200 μm diameter showed breakdown voltages (V_B) up to 7.5 kV for drift region carrier concentration of 8x10¹⁵ cm⁻³. This exceeds the unipolar 1D limit for SiC and was achieved without substrate thinning or annealing of the epi layer structure. The power figure-of-merit, V_B²/Ro_N, was 6.2 GW·cm⁻², where Ro_N is the on-state resistance (9.3-14.7 mΩ.cm²). The average electric field strength was 7.56 MV/cm, approaching the maximum for β-Ga₂O₃. The on-off ratio switching from 5 to 0V was 2x10¹³, while it was $3x10^{10}$ -2x10¹¹ switching to 100V. The turn-on voltage was in the range 1.9-2.1 V for the different contact diameters, while the reverse current density was in the range $2x10^{-8}$ -2x10⁻⁹ A.cm⁻² at -100V. The reverse recovery time was 21 ns, while the forward current density was >100 A/cm² at 5 V.

PLEASE CITE THIS ARTICLE AS DOI: 10.1116/6.0002580

I. INTRODUCTION

Recently, there has been major progress in advancing the technology of vertical geometry rectifiers based on monoclinic β -Ga₂O₃ ⁽¹⁻⁷⁾. Thick epitaxial layers grown on large area conducting substrates are commercially available, with manufacturing costs comparable or lower than SiC technology ⁽¹⁻³⁾. Breakdown voltages up to 8.32 kV with on-resistance 5.24 Ω . cm⁻² have been reported, producing a power figure-of-merit of 13.2 GW.cm⁻²⁽⁶⁾. Additional processing to reduce the drift region carrier density by extended annealing in O₂, followed by substrate thinning to reduce the on-resistance were needed to achieve these results ⁽⁶⁾. A recent report has demonstrated up to 6kV breakdown using a vertical structure with a deep trench of SiO₂ to provide edge termination ⁽⁷⁾. For the first time, these values exceed the unipolar limit of SiC and GaN power devices ⁽⁶⁻⁸⁾. While less desirable for power switching applications due to total current limitations, lateral β -Ga₂O₃-based devices with breakdown voltage up to 8 kV ⁽⁹⁻¹¹⁾ and critical breakdown fields also exceeding the theoretical electric field limits of SiC and GaN have been reported ^(10,11,12-14).

One of the innovations that have led to the high breakdown voltage is the use of NiO as a conducting p-type oxide to form vertical p-n heterojunctions with n-type Ga_2O_3 (4,6,8,15-30). Compared to the previous generation of Schottky rectifiers in Ga_2O_3 (12-14), these p-n junction devices show larger breakdown voltages with only a slight increase in turn-on voltages (15-29). Zhou et al. (29) give a detailed account of the design trade-offs. For example, a direct comparison of heterojunction and Schottky rectifiers fabricated on the same wafer showed breakdown voltage of 4.7 kV, power figure-of-merits, V_B^2/R_{ON} of 2 GW·cm⁻², and on-state resistance, R_{ON} , of 11.3 m Ω .cm² for the former (8), while Schottky rectifiers without the NiO showed V_B of 840 V and power figure-of-merit of 0.11 GW.cm⁻² (8). The bipolar transport available in such structures can induce both conductivity modulation and low on-resistance.

PLEASE CITE THIS ARTICLE AS DOI: 10.1116/6.0002580

In this letter, we demonstrate 7.5 kV V_B in vertical planar NiO/Ga₂O₃ rectifiers and FOM of 6.2 GW.cm⁻². These devices are processed without the complications of wafer thinning or annealing of the drift region to reduce the carrier concentration. This simplified processing sequence is attractive from a manufacturability viewpoint. Compared to previous reports with bilayer NiO ⁽²²⁾, we achieve higher V_B through the lower doping in the drift region, optimization of the NiO deposition process and simplified design without field limiting rings. In our own previous work we achieved 4.7kV V_B, but through use of the lower doping and optimized process, we achieve a significant improvement in breakdown voltage here and performance beyond the unipolar limit of GaN.

II. EXPERIMENTAL

A schematic of the vertical heterojunction rectifiers is shown in Figure 1. The drift region was a 10 μ m thick, lightly Si doped (8x10¹⁵ cm⁻³) layer grown by halide vapor phase epitaxy (HVPE) on a (001) surface orientation Sn-doped β -Ga₂O₃ single crystal (Novel Crystal Technology, Japan). Figure 2 shows the C-V data confirming the carrier density of 8x10¹⁵ cm⁻³ in the drift region. The full area Ti/Au back Ohmic contact was deposited by e-beam evaporation and annealed at 550 °C for 60s under a flowing N₂ ambient ^(30,31). The surface was cleaned by UV/Ozone exposure for 10 mins. The bilayer NiO was deposited by magnetron sputtering at 3mTorr and 80W of 13.56 MHz power at a final rate of 0.06 Å.sec⁻¹. The initial deposition is done at low powers (30W) to minimize surface damage. We also used the Ar/O₂ ratio (flow rates 5/15 sccm respectively) during sputtering to control the doping in the NiO. A 20/80 nm Ni/Au contact metal (50-200 μ m diameter) was deposited onto the NiO layer after annealing at 300°C under O₂ ambient ⁽⁸⁾. The NiO extends 3um beyond the contact metal, so the diameter is 6um larger. The devices are not isolated by trenches or dielectrics but are defined by the contacts.

The current-voltage (I-V) characteristics were recorded with a Tektronix 370-A curve tracer, 371-B curve tracer and Agilent 4156C was used for

PLEASE CITE THIS ARTICLE AS DOI: 10.1116/6.0002580

forward and reverse current characteristics $^{(30,31)}$. A Glassman power supply was used for the reverse characteristics. The reverse breakdown voltage was defined as the bias for a reverse current reaching 0.1 A.cm². The I-V characteristics were quite uniform over areas of 1 cm² on the wafer, with absolute currents within 15% at a given voltage. We tested 40 of the 100 μ m diodes and 25 of the 50 μ m. Of the 65 devices, 27 are above 7.5 kV V_B and 51 above 7kV with reverse currents within 20% of each other.

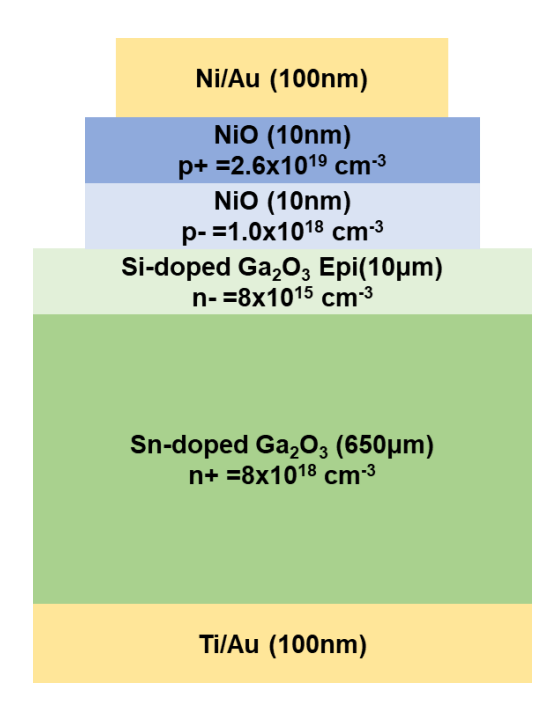


Figure 1. Schematic of NiO/Ga₂O₃ heterojunction rectifier.

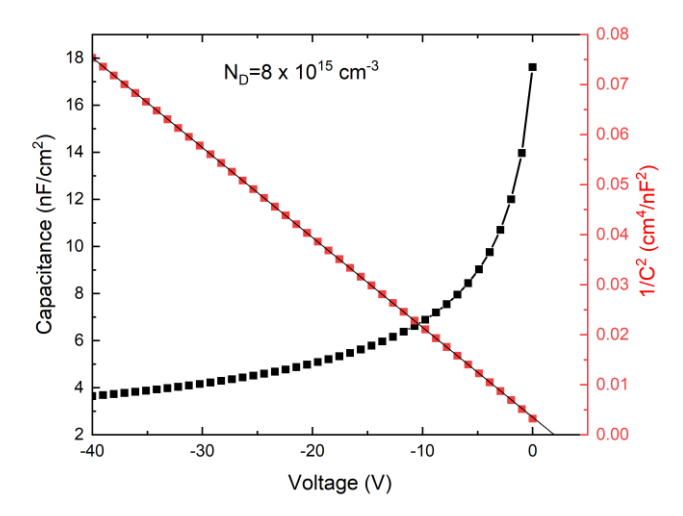


Figure 2. C-V characteristics for determining carrier density in drift region.

PLEASE CITE THIS ARTICLE AS DOI: 10.1116/6.0002580

III. RESULTS AND DISCUSSION

The forward J-V characteristics are shown in Figure 3 (a) for three different device diameters. The on-resistance was in the range 9.3-14.7 m Ω . cm⁻² with forward current densities > 100 A.cm⁻² at 5 V. The on-off ratio was $2x10^{13}$ for 5V/0V. The same data is shown in linear form in Figure 3(b), showing the turn-on voltage was in the range 1.9-2.1 V for the different device sizes.

The reverse I-V characteristics are shown in Figure 4 (a) for the devices fabricated on the 8x10¹⁵ cm⁻³ drift layers, as well our previous result of 4.7 kV obtained on higher doped drift regions (2x10¹⁶ cm⁻³) (8) Notice that the reduction in carrier density leads to a significantly higher breakdown voltage of 7.5 kV. These were measured in Fluorinert atmosphere at 25°C. It is noteworthy this was obtained without the need for annealing of the epi structure to further reduce carrier density or to thin the substrate to reduce on-resistance. The leakage increases sharply under biases <500V, we speculate in this design of NiO-based structures is due to the depletion width initially spreading sideways and leading to more leakage until the point where the edge of the NiO is reached and vertical depletion becomes dominant. The power figure of merit was 6.2 GW.cm⁻². This is still lower than the theoretical maximum of ~34 GW.cm⁻² (1,6) but shows the recent progress in material quality and edge termination design. The simplicity of this planar device design and processing sequence without trenches can reduce fabrication costs and improve yield. The rectifiers also have a high average electric field strength of $7.58 \text{ kV/}(0.02 \mu\text{m} + 10 \mu\text{m}) = 7.56 \text{ MV/cm}$, which is approaching the reported maximum near 8MV.cm⁻¹. The exact breakdown field strength is not fully addressed either theoretically or experimentally. Previous high breakdown devices have shown average

PLEASE CITE THIS ARTICLE AS DOI: 10.1116/6.0002580

fields from 6.2-6.5 MV/cm ⁽⁶⁾ and even as high as 6MV/cm in Schottky designs without the p-n junction ⁽⁷⁾. The critical field is defined as the maximum electric field that leads to avalanche breakdown in a 1D analytical model. For Ga₂O₃, there is as yet no experimental data confirming temperature-dependent behavior indicative of true avalanche breakdown. An extensive discussion in the certainties of establishing the true breakdown field in such circumstances have been given elsewhere ^(33,34). A key finding was that future development of UWBG materials is expected to change some critical field values ^(33,34).

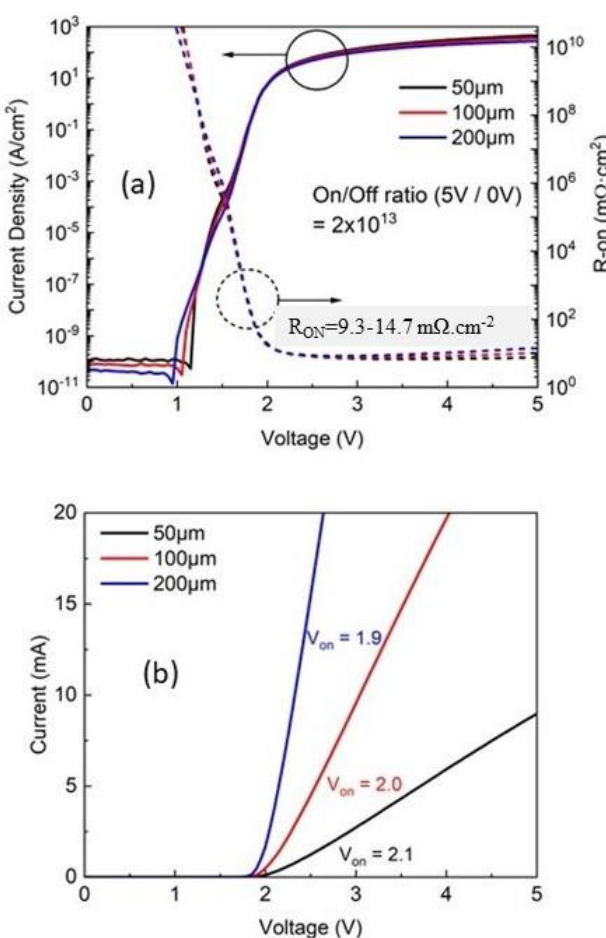


Figure 3. (a) Log plot of forward current densities and R_{ON} values (b) linear forward I-V characteristics of NiO/Ga₂O₃ heterojunction rectifiers.

PLEASE CITE THIS ARTICLE AS DOI: 10.1116/6.0002580

(a) 10^{0} $V_{B} = -4767 \text{ V}$ $V_{B} = -7586 \text{ V}$ FOM= 6.2 GW/cm² $V_{B} = -7586 \text{ V}$ $V_{B} = -7$

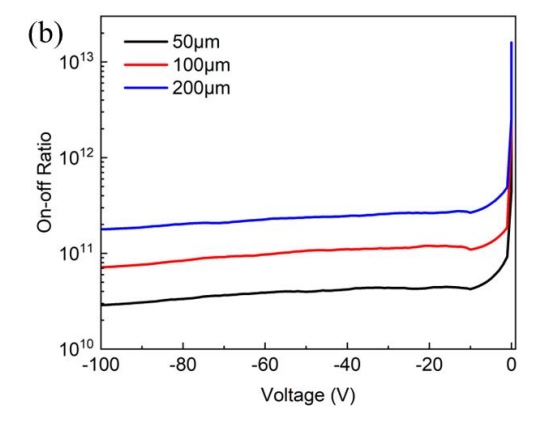


Figure 4. (a) Reverse I-V characteristics and breakdown voltage (b) On-off ratio of NiO/Ga₂O₃ heterojunction rectifiers in which the bias was switched from 5V forward to the voltage shown on the x-axis.

The on/off ratio when switching from 5V forward to the reverse bias on the x-axis is shown in Figure 4 (b) for the three different device sizes. The values are still in the range $3x10^{10}$ - $2x10^{11}$ when switching to 100V, showing the excellent rectification characteristics of the devices.

PLEASE CITE THIS ARTICLE AS DOI: 10.1116/6.0002580

(a) 100 **Pulse Condition:** Period = 50 μs Duty Cycle = 1 μs (20%) Power Supply = +10/-10 V Current (mA) $dI/dt = -3.2A/\mu s$ T_{rr} = 21 ns = 18 mA $I_F = 80 \text{ mA}$ 20 -20 100 700 200 300 400 500 600 Time (ns) Ga₂O₃ SBD/JBS NiO/Ga₂O₃ SiC This Work $R_{\text{on,sp}}$ (m Ω .cm²) NJU 20' Cornell 20' VIFL 22 ME Co 17' NICT 17' USTC SYSU 20'**.** NJU 21' 15'_{VT} 19'**.** XDU 20' 10⁰ XDU 21 **UT 21 XDU 22** 10^{3} 10⁴ $V_B(V)$

Figure 5. (a) Switching waveform for NiO/Ga_2O_3 heterojunction rectifiers (b) Compilation of Ron versus V_B of conventional and NiO/Ga_2O_3 heterojunction rectifiers reported in the literature.

Figure 5(a) shows the reverse recovery waveform when switching from 80 mA forward current to -10V. The details of the measurements have been reported previously ⁽³⁵⁾. The reverse recovery time is 21ns, showing that charge storage in the p-n junction is not significant.

Figure 5(b) shows a compilation of Ron versus V_B results reported in the literature for conventional Schottky barrier or JBS rectifiers and NiO/Ga₂O₃ heterojunction rectifiers, along with the theoretical lines for SiC, GaN and Ga₂O₃. The

PLEASE CITE THIS ARTICLE AS DOI: 10.1116/6.0002580

present work shows that Ga₂O₃ is now achieving results beyond the 1D unipolar limits of GaN and SiC. Continued progress on reduced defect density in the Ga₂O₃ epi layers and optimized edge termination schemes should establish that this material has significant potential in power switching applications.

The breakdown voltages we have obtained are roughly a factor of two larger than our previous report on epi layers with doping about 3 times higher. We have noticed lower extended defect density in these epi layers, indicating more optimized growth and also modified our process to employ lower biases during sputter deposition of the NiO, optimized the gas flow ratio during deposition and also the surface cleaning prior to the NiO deposition. All of these lead to higher breakdown voltage without degrading on-resistance and demonstrate the potential of p-NiO as a technique for junction engineering in β -Ga₂O₃ power devices (36,37). There is also interest in using p-NiO gates for normally-off Ga₂O₃ heterojunction field effect transistors (38). Finally, it is expected that uniformity of the wafers will improve. The trends of V_B across a wafer of the type we used have recently been published by Wang et al. (39).

IV. SUMMARY AND CONCLUSIONS

In summary, we report a NiO/ β -Ga₂O₃ p-n heterojunction rectifier with V_B 7.5 kV with R_{on} of 9.3 m Ω ·cm² and a figure-of-merit (V_b²/R_{on}) of 6.2 GW.cm⁻². This work shows that existing wafer and fabrication technology is now capable of consistently exceeding the unipolar power device performance of SiC.

ACKNOWLEDGMENTS

PLEASE CITE THIS ARTICLE AS DOI: 10.1116/6.0002580

The work at UF was performed as part of Interaction of Ionizing Radiation with Matter University Research Alliance (IIRM-URA), sponsored by the Department of the Defense, Defense Threat Reduction Agency under award HDTRA1-20-2-0002. The content of the information does not necessarily reflect the position or the policy of the federal government, and no official endorsement should be inferred. The work at UF was also supported by NSF DMR 1856662.

Data Availability

The data that supports the findings of this study are available within the article and its supplementary material.

Declarations

The authors have no conflicts to disclose

REFERENCES

¹M. H. Wong and M. Higashiwaki, IEEE T Electron Dev, 67, 3925 (2020).

² Andrew J. Green, James Speck, Grace Xing, Peter Moens, Fredrik Allerstam, Krister Gumaelius, Thomas Neyer, Andrea Arias-Purdue, Vivek Mehrotra, Akito Kuramata, Kohei Sasaki, Shinya Watanabe, Kimiyoshi Koshi, John Blevins, Oliver Bierwagen, Sriram Krishnamoorthy, Kevin Leedy, Aaron R. Arehart, Adam T. Neal, Shin Mou, Steven A. Ringel, Avinash Kumar, Ankit Sharma, Krishnendu Ghosh, Uttam Singisetti, Wenshen Li, Kelson Chabak, Kyle Liddy, Ahmad Islam, Siddharth Rajan, Samuel Graham, Sukwon Choi, Zhe Cheng, and Masataka Higashiwaki, APL Mater. 10, 029201 (2022).

³S. J. Pearton, Fan Ren, Marko Tadjer and Jihyun Kim, J. Appl. Phys. 124, 220901 (2018).

⁴Chenlu Wang, Jincheng Zhang, Shengrui Xu, Chunfu Zhang, Qian Feng, Yachao Zhang, Jing Ning, Shenglei Zhao, Hong Zhou and Yue Hao, J. Phys. D: Appl. Phys. 54, 243001 (2021).

⁵S. Sharma, K. Zeng, S. Saha, U. Singisetti, IEEE Electr Device L. 41, 6 836 (2020).

This is the author's peer reviewed, accepted manuscript. However, the online version of record will be different from this version once it has been copyedited and typeset. PLEASE CITE THIS ARTICLE AS DOI: 10.1116/6.0002580

⁶Jincheng Zhang, Pengfei Dong, Kui Dang, Yanni Zhang, Qinglong Yan, Hu Xiang, Jie Su, Zhihong Liu, Mengwei Si, Jiacheng Gao, Moufu Kong, Hong Zhou and Yue Hao, Nat Commun **13**, 3900 (2022).

⁷Pengfei Dong, Jincheng Zhang, Qinglong Yan, Zhihong Liu, Peijun Ma, Hong Zhou and Yue Hao, IEEE Electr Device L, 43, 765 (2022).

⁸Jian-Sian Li, Chao-Ching Chiang, Xinyi Xia, Timothy Jinsoo Yoo, Fan Ren, Honggyu Kim, and S. J. Pearton, Appl. Phys. Lett. 121, 042105 (2022).

⁹S. Roy, A. Bhattacharyya, P. Ranga, H. Splawn, J. Leach and S. Krishnamoorthy, IEEE Electr Device L. 42, 1140 (2021).

¹⁰Arkka Bhattacharyya, Shivam Sharma, Fikadu Alema, Praneeth Ranga, Saurav Roy, Carl Peterson, Geroge Seryogin, Andrei Osinsky, Uttam Singisetti and Sriram Krishnamoorthy, Appl. Phys. Express **15**, 061001(2022).

¹¹K. D. Chabak, K. D. Leedy, A. J. Green, S. Mou, A. T Neal, T. Asel, E. R. Heller,
N. S. Hendricks, K. Liddy, A. Crespo, N. C. Miller, M. T. Lindquist, N. Moser, R.
C. Fitch Jr, D. E. Walker Jr, D. L Dorsey and G. H. Jessen, Semicond Sci Tech, 35,
013002 (2020).

¹²Zongyang Hu, Kazuki Nomoto, Wenshen Li, Zexuan Zhang, Nicholas Tanen, Quang Tu Thieu, Kohei Sasaki, Akito Kuramata, Tohru Nakamura, Debdeep Jena, and Huili Grace Xing, Appl. Phys. Lett. 113, 122103 (2018).

¹³Ribhu Sharma, Minghan Xian, Chaker Fares, Mark E. Law, Marko Tadjer, Karl D. Hobart, Fan Ren and Stephen J. Pearton, J. Vac. Sci. Technol A 39, 013406 (2021).

¹⁴Wenshen Li, Devansh Saraswat, Yaoyao Long, Kazuki Nomoto, Debdeep Jena, and Huili Grace Xing, Appl. Phys. Lett. 116, 192101 (2020).

¹⁵Y. Lv, Y. Wang, X. Fu, Shaobo Dun, Z. Sun, Hongyu Liu, X. Zhou, X. Song, K. Dang, S. Liang, J. Zhang, H. Zhou, Z. Feng, S. Cai and Yue Hao, IEEE T Power Electr. 36, 6179 (2021).

¹⁶Ming Xiao, Boyan Wang, Jingcun Liu, Ruizhe Zhang, Zichen Zhang, Chao Ding, Shengchang Lu, Kohei Sasaki, Guo-Quan Lu, Cyril Buttay and Yuhao Zhang, IEEE T Power Electr 36, 8565 (2021).

This is the author's peer reviewed, accepted manuscript. However, the online version of record will be different from this version once it has been copyedited and typeset.

PLEASE CITE THIS ARTICLE AS DOI: 10.1116/6.0002580

¹⁷X. Lu, Xianda Zhou, Huaxing Jiang, Kar Wei Ng, Zimin Chen, Yanli Pei, Kei May Lau and Gang Wang, IEEE Electr Device L.41, 449 (2020).

¹⁸Chenlu Wang, Hehe Gong, Weina Lei, Y. Cai, Z. Hu, Shengrui Xu, Zhihong Liu, Qian Feng, Hong Zhou, Jiandong Ye, Jincheng Zhang, Rong Zhang, and Yue Hao, IEEE Electr Device L, 42, 485 (2021).

¹⁰Qinglong Yan, Hehe Gong, Jincheng Zhang, Jiandong Ye, Hong Zhou, Zhihong Liu, Shengrui Xu, Chenlu Wang, Zhuangzhuang Hu, Qian Feng, Jing Ning, Chunfu Zhang, Peijun Ma, Rong Zhang, and Yue Hao, Appl. Phys. Lett. 118, 122102 (2021).

²⁰H. H. Gong, X. H. Chen, Y. Xu, F.-F. Ren, S. L. Gu and J. D. Ye, Appl. Phys. Lett., 117, 022104 (2020).

²¹Hehe Gong, Feng Zhou, Weizong Xu, Xinxin Yu, Yang Xu, Yi Yang, Fang-fang Ren, Shulin Gu, Youdou Zheng, Rong Zhang, Hai Lu and Jiandong Ye, IEEE T Power Electr., 36, 12213 (2021).

²²H. H. Gong, X. X. Yu, Y. Xu, X. H. Chen, Y. Kuang, Y. J. Lv, Y. Yang, F.-F. Ren,
Z. H. Feng, S. L. Gu, Y. D. Zheng, R. Zhang, and J. D. Yue, Appl. Phys. Lett. 118,
202102 (2021).

²³W. Hao, Q. He, K. Zhou, G. Xu, W. Xiong, X. Zhou, G. Jian, C. Chen, X. Zhao, and S. Long, Appl. Phys. Lett., 118, 043501 (2021).

²⁴F. Zhou, Hehe Gong, Weizong Xu, Xinxin Yu, Yang Xu, Yi Yang, Fang-fang Ren, Shulin Gu, Youdou Zheng, Rong Zhang, Jiandong Ye and Hai Lu, IEEE T Power Electr, 37, 1223 (2022).

²⁵Qinglong Yan, Hehe Gong, Hong Zhou, Jincheng Zhang, Jiandong Ye, Zhihong Liu, Chenlu Wang, Xuefeng Zheng, Rong Zhang, and Yue Hao, Appl. Phys. Lett. 120, 092106 (2022).

²⁶Y. J. Lv, Y. G. Wang, X. C. Fu, S. B. Dun, Z. F. Sun, H. Y. Liu, X. Y. Zhou, X. B. Song, K. Dang, S. X. Liang, J. C. Zhang, H. Zhou, Z. H. Feng, S. J. Cai, and Y. Hao, IEEE T Power Electron. 36, 6179 (2021).

PLEASE CITE THIS ARTICLE AS DOI: 10.1116/6.0002580

²⁷Jiaye Zhang, Shaobo Han, Meiyan Cui, Xiangyu Xu, Weiwei Li, Haiwan Xu, Cai Jin, Meng Gu, Lang Chen and Kelvin H. L. Zhang, ACS Appl. Electron. Mater. 2, 456 (2020).

²⁸Yuangang Wang, Hehe Gong, Yuanjie Lv, Xingchang Fu, Shaobo Dun, Tingting Han, Hongyu Liu, Xingye Zhou, Shixiong Liang, Jiandong Ye, Rong Zhang, Aimin Bu, Shujun Cai and Zhihong Feng, IEEE T Power Electr. 37, 3743 (2022).

²⁹Hong Zhou, Shifan Zeng, Jincheng Zhang, Zhihong Liu, Qian Feng, Shengrui Xu, Jinfeng Zhang and Yue Hao, Crystals 11, 1186 (2021).

³⁰ Boyan Wang; Ming Xiao; Joseph Spencer; Yuan Qin; Kohei Sasaki; Marko J. Tadjer; Yuhao Zhang, IEEE Electr Device L 44, 221 (2023).

³¹Jiancheng Yang, Minghan Xian, Patrick Carey, Chaker Fares, Jessica Partain, Fan Ren, Marko Tadjer, Elaf Anber, Dan Foley, Andrew Lang, James Hart, James Nathaniel, Mitra L. Taheri, S. J. Pearton and Akito Kuramata, Appl. Phys. Lett. 114, 232106 (2019).

³²J. Yang, F. Ren, Y.-T. Chen, Y.-T. Liao, C.-W. Chang, J. Lin, M. J. Tadjer, S. J. Pearton, and A. Kuramata, IEEE J. Electron Devi., 7, 57 (2019).

³³ Robert Kaplar, Oleksiy Slobodyan, Jack Flicker, Jeramy Dickerson, Trevor Smith, Andrew Binder and Mark Hollis, A New Analysis of the Dependence of Critical Electric Field on Semiconductor Bandgap, Electrochemical Society Meeting Abstracts 236, 1334-1334 (ECS Meeting, Atlanta, GA, Oct 2019).

³⁴ Oleksiy Slobodyan, Jack Flicker, Jeramy Dickerson, Jonah Shoemaker, Andrew Binder, Trevor Smith, Stephen Goodnick, Robert Kaplar and Mark Hollis Analysis of the dependence of critical electric field on semiconductor bandgap. J. Materials Res. 37, 849 (2022).

³⁵ Jian-Sian Li, Chao-Ching Chiang, Xinyi Xia, Fan Ren and S. J. Pearton, J. Vac Sci Technol A 40, 063407 (2022).

³⁶ W. Hao, Q. He, X. Zhou, X. Zhao, G. Xu and S. Long, "2.6 kV NiO/Ga₂O₃ Heterojunction Diode with Superior High-Temperature Voltage Blocking Capability," 2022 IEEE 34th International Symposium on Power Semiconductor Devices and ICs (ISPSD), Vancouver, BC, Canada, 2022, pp. 105-108.

PLEASE CITE THIS ARTICLE AS DOI: 10.1116/6.0002580

Weibing Hao, Feihong Wu, Wenshen Li, Guangwei Xu, Xuan Xie, Kai Zhou, Wei Guo, Xuanze Zhou, Qiming He, Xiaolong Zhao, Shu Yang and Shibing Long, "High-Performance Vertical β-Ga₂O₃ Schottky Barrier Diodes Featuring P-NiO JTE with Adjustable Conductivity," 2022 International Electron Devices Meeting (IEDM), San Francisco, CA, USA, 2022, pp. 9.5.1-9.5.4.

- ³⁸ X. Zhou, Q. Liu, W. Hao, G. Xu and S. Long, "Normally-off β-Ga₂O₃ Power Heterojunction Field-Effect-Transistor Realized by p-NiO and Recessed-Gate," 2022 IEEE 34th International Symposium on Power Semiconductor Devices and ICs (ISPSD), Vancouver, BC, Canada, 2022, pp. 101-104.
- ³⁹ Boyan Wang, Ming Xiao, Joseph Spencer, Yuan Qin, Kohei Sasaki, Marko J. Tadjer and Yuhao Zhang, IEEE Electr Device L, 44, 221 (2023).



Journal of Vacuum Science & Technology A

ACCEPTED MANUSCRIPT

This is the author's peer reviewed, accepted manuscript. However, the online version of record will be different from this version once it has been copyedited and typeset.

PLEASE CITE THIS ARTICLE AS DOI: 10.1116/6.0002580

Ni/Au (100nm)

NiO (10nm) p+ =2.6x10¹⁹ cm⁻³

NiO (10nm) p-=1.0x10¹⁸ cm⁻³

Si-doped Ga₂O₃ Epi(10µm) n-=8x10¹⁵ cm⁻³

Sn-doped Ga_2O_3 (650µm) n+ =8x10¹⁸ cm⁻³

Ti/Au (100nm)

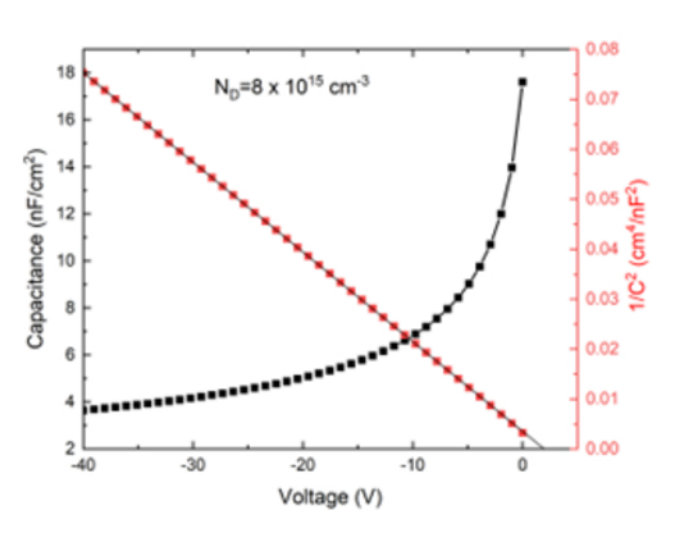


Journal of Vacuum Science & Technology A

ACCEPTED MANUSCRIPT

This is the author's peer reviewed, accepted manuscript. However, the online version of record will be different from this version once it has been copyedited and typeset.

PLEASE CITE THIS ARTICLE AS DOI: 10.1116/6.0002580

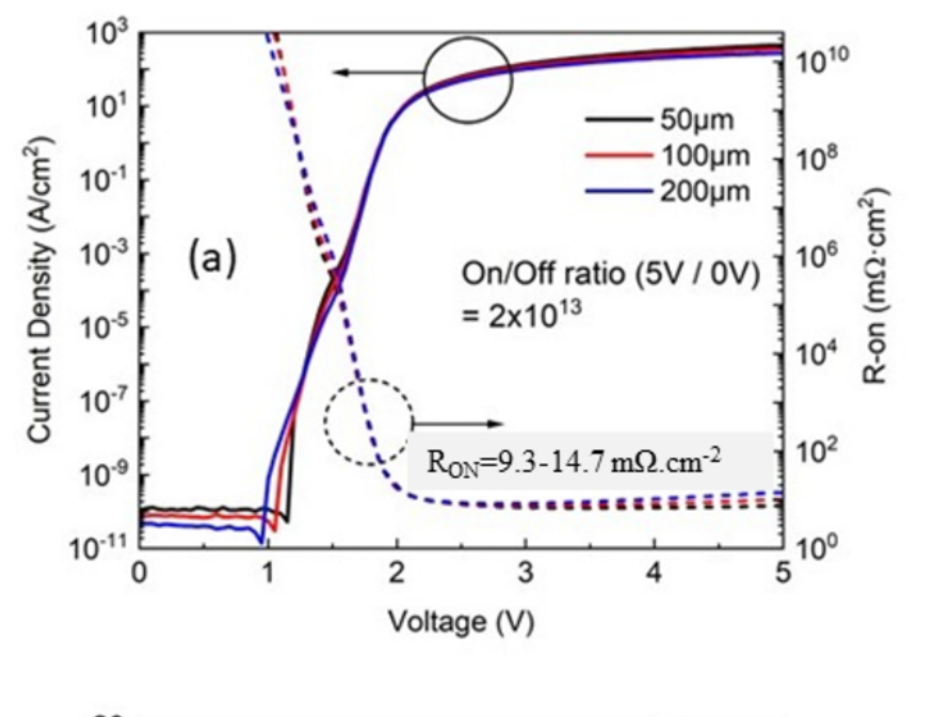


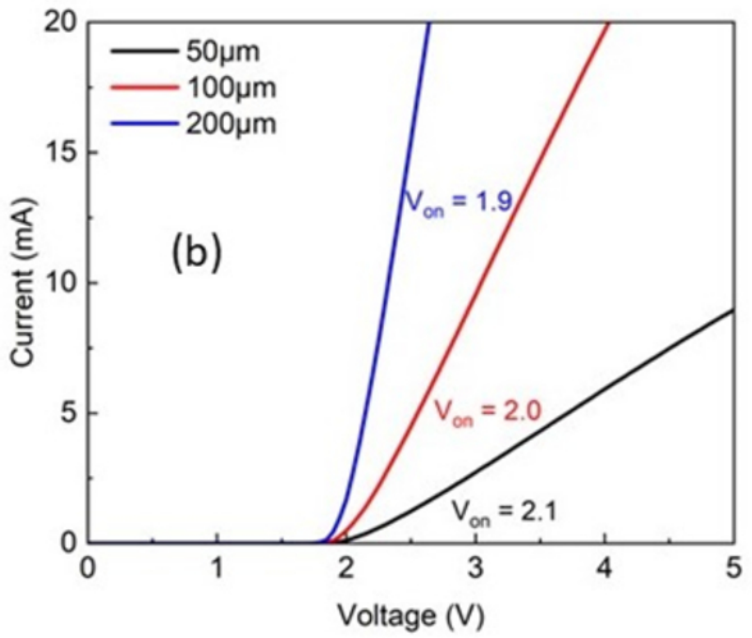


Technology A Vacuum Journal of N

ACCEPTED MANUSCRIPT







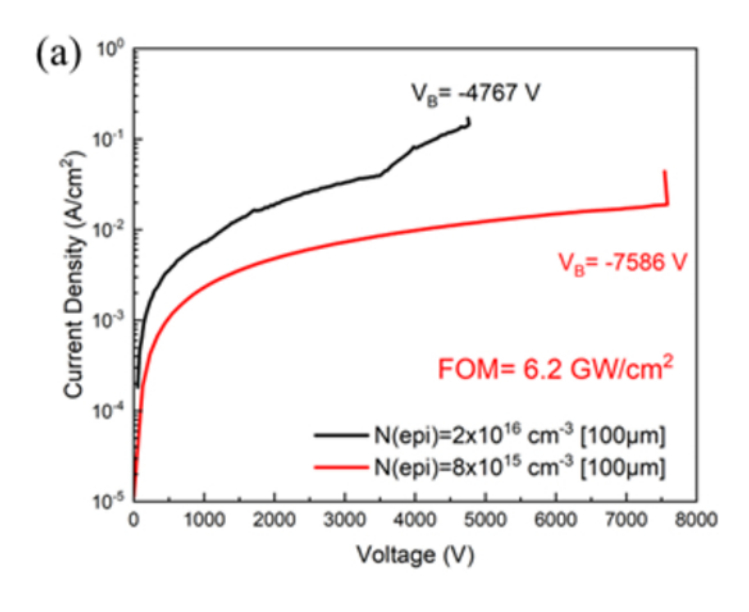
ACCEPTED MANUSCRIPT

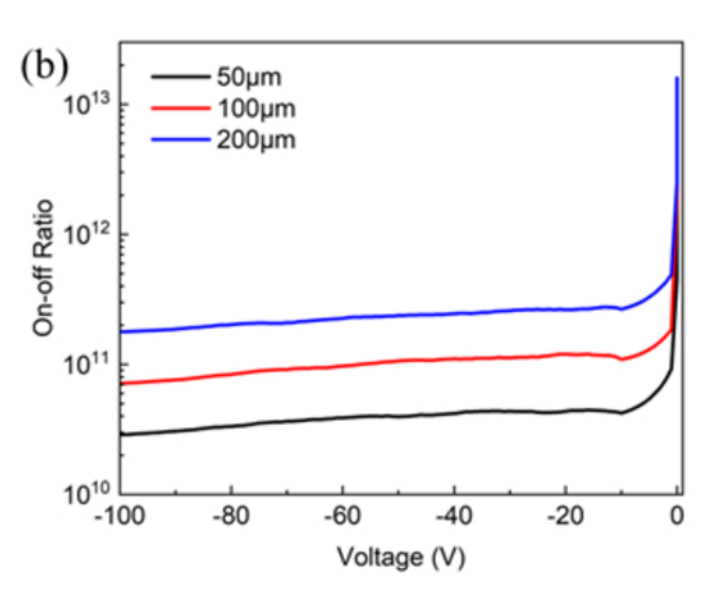
Journal of Vacuum Science & Technology A



This is the author's peer reviewed, accepted manuscript. However, the online version of record will be different from this version once it has been copyedited and typeset.

PLEASE CITE THIS ARTICLE AS DOI: 10.1116/6.0002580





ACCEPTED MANUSCRIPT

Technology Vacuum Science Journal



This is the author's peer reviewed, accepted manuscript. However, the online version of record will be different from this version once it has been copyedited and typeset.

PLEASE CITE THIS ARTICLE AS DOI: 10.1116/6.0002580

